UCRL-JC-129546
PREPRINT

Striped Double Cavity Fabry-Perot Interferometers Using Both Glass and Air Cavities

D. Goosman, L. Steinmetz, S. Perry

This paper was prepared for submittal to the
International Congress on High Speed Photography and Photonics
Moscow, Russia
September 20-25, 1998

July 8, 1998

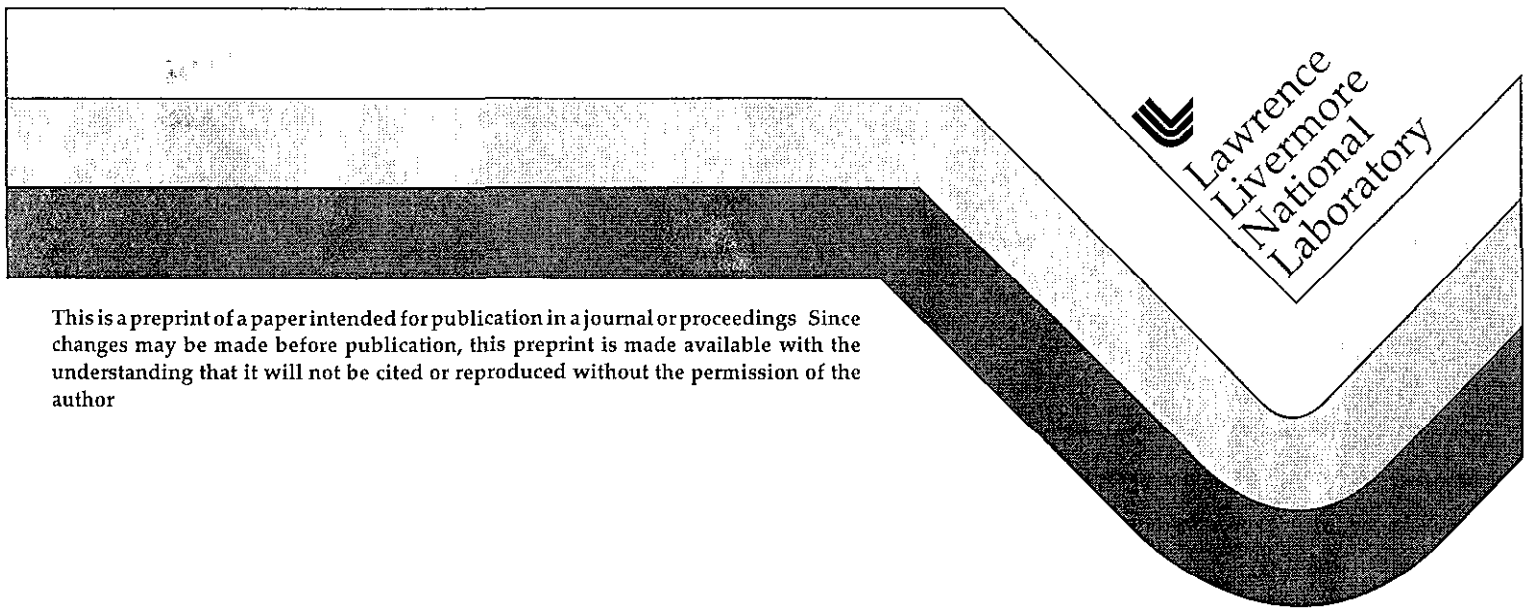

Submit to ICHSSP-98

Striped Double Cavity Fabry-Perot Interferometers Using Both Glass and Air Cavities

David Goosman, Lloyd Steinmetz and Stephen Perry

The authors are with Lawrence Livermore National Laboratory
P O Box 808, L-281, Livermore, CA 94550
925-422-1630, fax 925-422-2382

We have used piezo-driven Fabry-Perot interferometers in the past for many continuous velocity-time measurements of fast moving surfaces In order to avoid the annoying drift of some of these devices, we have developed and used inexpensive, solid glass, striped etalons with lengths up to 64 mm Useable apertures are 35 mm by 80 mm with a finess of 25 A roundabout technique was devised for double cavity operation We built a passive thermal housing for temperature stability, with tilt and height adjustments

We have also developed and used our first fixed etalon air-spaced cavity with a rotatable glass double-cavity insert. The rotation allows the referee cavity fractional order to be adjusted separately from that of the main cavity It needs very little thermal protection, and eliminates the need for a roundabout scheme for double cavity operation, but is more costly than the solid glass version

For a cavity with an air length H, glass length T, index n and wavelength λ, the fringe angles are

$$\sqrt{j\lambda/(H+T/n)}$$

where j is the fractional order plus an integer This means double cavity fringe patterns plotted vs velocity will cross if both air and glass are part of the system This crossing, which is an advantage, will not occur for pure glass or pure air systems The velocity per fringe is given by

$$\frac{c\lambda}{4(H+T(n-\lambda dn/d\lambda))}$$

where $dn/d\lambda$ is the derivative of index with respect to wavelength This expression therefore includes the effects of dispersion in the glass Because the angle depends upon T/n and the velocity upon Tn, there is no equivalent air cavity for a given glass cavity Very high quality glass is preferable to air, since for a given velocity per fringe, the fringe separation is larger for glass cavities, resulting in less finess degradation due to streak camera spatial resolution

Keywords velocimetry, double cavity, glass etalons

1 INTRODUCTION

Optical velocimetry is used at LLNL to measure the time dependent velocity of surfaces accelerated by gas guns, exploding foils and explosives(1) We have used both VISAR and Fabry-Perot interferometer systems for this purpose Since the Fabry systems can handle more than one frequency of return light, our team has used those systems exclusively for the last 15 years This is because some experiments have unDoppler shifted light arising from dust on windows or cross talk between fibers as well as shifted light Others have more than one source of shifted light For example, metal surfaces covered with transparent windows may have a shock wave in the window material which reflects and shifts some of the light differently than the shift due to the metal-window interface Although the reflectance from such shocks may be only a few percent, it may be more specular than the diffuse metal-window interface, which may reflect 60% of the light Thus the ratio of window-shock shifted light to metal interface light may be very significant Optical fibers carrying excessive laser power may induce stimulated Brillioun scattering,

which produces a second frequency of illumination light, which we have seen on Fabry records Some surfaces have been observed with our systems where half of the illuminated spot spalls and coasts whereas the rest of the spot decelerates, producing two separate Doppler shift histories

Our new manybeam velocimeter system (2) was described briefly at the last Congress and is shown in Figure 1, at which time we had 10 of the 20 channels of recorders in use We now have 15 recorder capability This systems has a cross talk between channels of less than 0 1%, but if one channel is many times brighter than the conjugate channel, the cross talk can be observed on the Fabry records This is another example of why we feel multiple frequency recording capability is needed for our velocimetry

Fabry systems are inherently more expensive than VISAR, and the interferometer is the heart of the system We have purchased or designed and used several types of interferometers We modified several piezo-driven interferometers to accommodate 70 mm diameter beams for our manybeam system, but have been unable to significantly reduce their inherent drift They produce excellent finesse for short periods of time

In a previous Congress (3) we reported results from our Versions I and II double cavity interferometers Version I used the mirror plates themselves as additional optical path to provide a second cavity Version II used a slab of glass optically contacted onto a commercial piezo driven system Version II has been used successfully for 4 years at LLNL In the last Congress our description of the manybeam velocimeter mentioned briefly our Version III interferometer, which has a separate glass slab inserted into part of a fixed air-spaced interferometer

In this report, we elaborate on the Version III system, both with fixed and piezo driven etalons, as well as our version IV system, which is a solid glass double cavity configuration

2 THEORY OF FABRY PEROT INTERFEROMETERS WITH BOTH GLASS AND AIR

Figure 2 shows a cavity containing a length H of air and a length T of glass, with the highly reflective surfaces being the ones at the left and right The optical path difference between two rays entering at angle theta is expressed as a multiple m of λ, so that

$$2nT/\cos(\text{theta}') + 2H/\cos(\text{theta}) - W\sin(\text{theta}) = m\lambda \qquad (1)$$

In general m is not an integer, but if it is, then m is the order of interference and theta is a resonant angle For theta = 0,

$$2nT + 2H = m_0\lambda = (m_1 + \varepsilon)\lambda \qquad (2)$$

where $m_1 = \text{INT}((2nT+2H)/\lambda)$ and ε is between 0 and 1 If $\varepsilon = 0$, then 0 degrees is a resonant angle

Using the small angle approximation for theta, it is straightforward from Fig 2 and Eqs (1) and (2) to show that the resonant angles are given by

$$\text{theta}_k = \sqrt{(k-1+\varepsilon)\lambda/(H+T/n)} \qquad (3)$$

Where the $k = m_1-m+1$, and Thetak is the kth fringe from the center of the pattern This is to be compared with the usual expression,

$$\text{theta}_j = \sqrt{j\lambda/H} \qquad (4)$$

Where, as described in Ref 2, j is the non-integer fringe number

We now derive the general expression for the velocity per fringe As the velocity increases but not so much that a new fringe evolves from the center of the fringe pattern, the resonant angle Theta_k of Eqn (3)

increases due to changes in both λ and ε, as well as n In this case, the order of interference m does not change and m_1 remains the same, = INT((2nT+2H)/λ) λ changes very slightly, typically by a few ppm, but the fractional order, ε , given by

$$\varepsilon = (2nT+2H)/\lambda - INT((2nT+2H)/\lambda), \tag{5}$$

changes signficantly Neglecting for now the variation of n with λ, we derive the velocity per fringe expression Figure 3 shows the fringe pattern before (λ) and after (λ') a small velocity increase By assumption of a small velocity increase , k' = k and $m_1' = m_1$ We construct the usual ratio of differences in theta^2 by using Eqn (3) to deduce that

$$(theta_k(\lambda')^2 - theta_k(\lambda)^2)/(theta_{k+1}(\lambda)^2 - theta_k(\lambda)^2) = ((k-1)(\lambda'-\lambda) + \lambda'\varepsilon(\lambda') - \lambda\varepsilon(\lambda))/\lambda, \tag{6}$$

which reduces to $4V/(c\lambda)*(H+nT)$, since $\lambda'-\lambda = -2\lambda V/c$, and $|1-k| << m_1$ In the final step we have also used the approximation that INT((2H+2nT)/λ) = (2H+2nT)/λ, since for H > 1 cm and λ = 5e-5 cm, the error in doing so is < 1/40000 Thus the velocity per fringe V_{fsr} is, as expected,

$$V_{fsr} = c\lambda/(4(H+nT)) \quad \text{(for no dispersion)} \tag{7}$$

It is straightforward to show that when the velocity jumps more than one free spectral range, the same derivation as above gives the same result, except that an integer is added to the left hand side of Eqn (6)

It is important to note that the velocity formula depends upon nT, whereas the angle formula depends upon T/n Because of this, there is no solid glass cavity length T which is equivalent in both velocity and angle to another pure air cavity of any length. This means that plots of fringe angle vs velocity for air+glass double cavity interferometers will cross, as shown in figure 4 In contrast, double cavity systems where both the main and referee cavities are solid glass or both are air only will have patterns that do not cross, as illustrated in figure 5

3 MODIFICATION OF THE VELOCITY FORMULAE FOR DISPERSION IN GLASS

The derivation of Eqn (7) neglected the very slight variation of the index n with the slight change in λ Barker (4) first pointed out for VISAR interferometer systems that this correction was not negligible In order to derive the correction for Fabry-Perot interferometers, one again uses Eqn (3), but this time allowing n to depend upon λ, assuming a linear dependence

$$n(\lambda') = n_0(\lambda) + (\lambda'-\lambda)dn/d\lambda \tag{8}$$

The same procedure, after several steps, yields the general velocity per fringe

$$V_{fsr} = c\lambda/(4(H+T(n_0-\lambda dn/d\lambda)), \tag{9}$$

Thus the effective index is changed by the dispersion For fused silica and green light, $\lambda dn/d\lambda$ = -0 024 The correction formula for Fabry-Perot systems is different from that for VISAR systems Note that in Eqn (3), the index n and ε are to be evaluated for the λ being considered However, for purposes of evaluating the fringe angle, either n(λ') or n_0 can be used, since they differ by only 0 05V/c for fused silica and green light Note that for V = 2 mm/usec, the real index difference is only 0 0000003, whereas the effective index change in the velocity formula is -0 024 for any velocity

For theta = 0 degrees, the derivation of the dispersion correction is simple Assume λ and λ' are both resonant at theta = 0, and that no wavelengths between them are also resonant at 0 deg Then

$$2(H+n(\lambda)T) = m_0*\lambda \quad \text{and} \quad 2(H+n(\lambda')T) = \lambda'(m_0+1) \tag{10}$$

Subtracting these two and using Eqn (8), along with $\lambda' = \lambda(1-2V/c)$ and $m_0 = 2(H+n(\lambda)T)/\lambda$, gives the same result as Eqn (9) We have verified the accuracy of Eqn (9) experimentally to better than 1% in velocity by using double cavity systems with main cavities consisting of air only, and referee cavities consiting of both glass and air to measure the same velocity It may be possible for some materials, however, to have a sharp change in index near λ which is so sharp that it is not reported in the literature This unlikely situation would invalidate Eqn (9)

With the above equations, one can show that for pure air or pure glass cavities of index n_0, the fringe angle expressed as a function of target velocity is given by

$$\text{theta}(V) = 2\sqrt{(V-V_0)/c*(n_0^2-\lambda_0 n_0 dn/d\lambda)} \tag{11}$$

Where V_0 is the velocity for which the fringe angle is 0 for the same order of intereference This means that the various curves of figure 5 have the same slopes, and that the slope, dTheta/dV, is independent of T or H, as long as the cavity is pure air or pure glass, and is not a combination of glass and air Therefore, if one expects a particular velocity jump in an experiment, one cannot make the change in theta larger by making H or T larger, even though this change would make the velocity per fringe smaller

It is interesting to compare a pure air etalon with a pure glass etalon of equal finesse and with H = T The glass one is better for two reasons Firstly the velocity per fringe is lower by a factor of n and therefore the velocity resolution determined by the etalon is better by the same factor In addition, the fringe angles are larger by a factor of $\sqrt{n}$, meaning that the spatial resolution of the streak camera recording the fringe pattern is not as significant in degrading the total velocity resolution It is not the same to increase the focal length of the lens after the etalon to increase the fringe diameters at the slit of the camera This is because it also increases the horizontal magnification (unless the lens is replaced by two cylinder lenses) which reduces the fraction of light that can pass through the slit of the streak camera, as outlined in ref 1

Reference 1 gave equations for velocity and time resolution for complete Fabry-Perot velocimeter systems These equations are easily generalized to mixtures of air and glass cavities by the following recipe

In formulae involving fringe angles, q values or finesses, replace H by $H + T/n_0$

In formulae involving velocities or time resolutions, replace H by $H + T*(n_0-\lambda_0 dn/d\lambda)$

4 VERSION 3 FIXED ETALON WITH REMOVABLE GLASS INSERT

Figure 6 shows our first version 3 interferometer It consists of two mirrors, each of 70 mm diam clear aperture, coated to 99 5% and 93% reflectivity, respectively, mounted on three zerodur pillars The 99 5% mirror was striped as described in Ref 2 by us, and the etalon was then assembled by TecOptic, Inc to sufficient parallelism to provide a finesse of 23 The housing has a slot which allows insertion of various glass plates to increase cavity length for a referee cavity The glass insert can be rotated about the vertical axis by a few degrees to adjust the fractional order of the referee cavity without changing the fractional order of the main cavity This adjustment is very useful for actual dynamic experiments to keep the referee lines as much as possible out of the region of interest in the fringe pattern

We have two fixed etalon interferometers, one with the insert capability The advantages of version 3 is that they are relatively insensitive to thermal effects and other sources of drift In contrast to the version 2 system, they can be used in remote locations because they do not drift, and can be made into single cavity systems simply by removing the insert

We found these to be so useful that we designed and used an insert capability for our conventional piezo-driven interferometers Figure 7 shows our system for holding inserts ranging from 9mm to 30 mm thick.

5 VERSION 4 FIXED ETALON SOLID BLOCKS

Our first good fixed etalon did not have the insert capability, so we developed a solid glass block interferometer to be used as a referee cavity in a round-about configuration shown in figure 8 The separator and recombiner mirrors need to be flat out to the edge of the mirror For the recombiner mirror, which is bevelled, we found it necessary to have the mirror blank bevelled first, then ground flat and polished and coated, in order to minimize distortions near the edge

The high cost of the fixed etalon systems encouraged us to see if solid etalons could be made good enough to provide a referee cavity, since the finesse of the referee does not have to be as high as that of the main cavity We chose fused silica, with n = 1 46, because it could be obtained with an index homogeneity of better than 1 ppm However, it is easy to show that for a solid block 64 mm deep, the homogeneity must be <0 2 ppm to make the required finesse of about 20

Three solid blocks 60 mm wide and 80 mm high, with depths of 64, 53 and 53 mmof Corning 7940 glass were fabricated for us by Bond Optics, Inc , with a specification of $\lambda/30$ for parallelism We tested these prior to coating by inserting them into an adjustable-air spaced piezo-driven cavity, such that the transmission pattern for parallel light could be viewed on a white card It was crucial to insulate the interferometer for thermal effects and wait about 60 minutes after handling to make measurements, since heat from finger contact persists in the block By viewing parts of the pattern on the two sides and top of the block, where only an air cavity existed, we could adjust the external mirrors to parallelism Then by moving the common piezo control to change the mirror spacing, we could infer the quality of the block by whether or not the pattern through it and the air moved as the common knob was changed The ideal block would resonate all at once, illuminating the entire area with one setting

If the index homogeneity were perfect, this intracavity test prior to coating is not very sensitive to parallelism errors, since if the block is a bit thicker at the bottom than at the top, then the air length in this arrangement is a bit thinner at the bottom The sensitivity here is 3 times less than when the block is reflectively coated

Despite the 1 ppm homogeniety specification being 5 times what we needed, we were pleased to find that these blocks were much more homogeneous than 1 ppm over a rectangular region 8 cm high and about 4 cm wide The two 1 cm wide edges running vertically did not resonate at the same setting as the center 4 cm did. The two edges did not resonate because of a variation of the nT product, and we were unable to distinguish between changes in n and changes in T But 4 cm width for the quality area is more than enough for a referee cavity, and almost enough for a main cavity, so we designed and built the housing shown in figure 9

The major problem with solid etalons of fused silica is the variation of the index with temperature, because for green light dn/dt = 1 0E-5 per deg C One needs to keep the bottom and top of the block within 0 02 deg C in order to keep the optical paths sufficiently close The block rests on a thermally insulating ceramic foam and is surrounded by about 8 kg of copper on 5 sides to act as a thermal mass The outside of the copper is surrounded on five sides by metallic-covered bubble insulation with an R value of 8 The input and output light each pass through a double-pane window of antireflection-coated optical plates Two-axis tilt and height control is provided by thin shafts and knobs which protrude outside the insulation, for ease of adjustment The height control is needed since the upstream mirror was striped.

Used in the round-about configuration, this solid referee block has been successfully used in dynamic experiments If the blocks are good enough, the cost is much less than the Version III systems Each of the three blocks was good enough to be a referee cavity However, we purchased 4 more blocks of a different glass, and have not yet been successful in making a very good interferometer

Although the 64 mm deep solid etalons need intensive thermal isolation, the solid fused-silica inserts used in the version 3 systems need less insulation, because the glass length is typically only 30% of the air length dn/dT for fused silica is 1 0E-5 per deg C, and the expansion coefficient, dL/dT is 5E-7 per deg C

The three successful etalons have the following properties operating in the striped configuration

Block depth (mm)	Aperture width (mm)	Finesse	J value
53 16	25	32	0 35
		28	0 74
		26	0 94
		22	1 35
		21 5	1 74
		17	1 94
53 16	40	30	0 5
		22	1 5
64 34	30	21	1 1
	25	32	0 4
		22	1 3

Low J values have higher finesse because they sample less of the height of the block.

The last block was tested for temperature sensitivity in its themal housing by measuring the finesse of the j=1 5 fringe starting at equilibrium with the room temperature at 70 deg F Then the room air temperature was increased by about 1 deg F per minute to 80 deg F , and then held for 8 minutes There was no significant change in the finesse, indicating the thermal housing was sufficient

For the striped solid etalons, we set the full width of the stripe so that

$$\text{Stripe full-width} = 4*\sqrt{(\lambda T/n)} \qquad (12)$$

to match the standard condition (Ref 5) which is set up so that, if there were no diffraction, all of the j=4 light and half of the j=1 light would be multiply reflected. For mixed air-glass cavities, we set the stripe width on the external mirrors appropriately for the main (air) cavity, i e , $= 4\sqrt{(\lambda H)}$

6 SUMMARY OF THE VARIOUS TYPES OF INTERFEROMETERS

The table below lists advantages and disadvantages for the various types of double cavity interferometers we use They are

Version 1 – one mirror is partially coated on both sides of the plate – described in Ref 3

Version 2 - the downstream mirror has a referee step optically contacted – described in Ref 3

Version 3 - a fixed air-spaced main cavity with a glass insert referee

Version 4 - a pair of solid glass etalons or a solid referee and a fixed main cavity in a round-about configuration (Figure 8)

Version 5 – a commercial piezo-driven system with an LLNL designed glass insert referee

Version	Cost	Performance	Advantages	Disadvantages
1	Mod	Marginal	Simple	Performance
2	High	Very good	Simple, adjustable spacing	Drifts
3	High	Very good	Can run remotely Can vary T, ε ref	Main cavity length fixed
4	Mod	Good	Can run remotely	Needs thermal housing
5	Mod	Good	H,T, both ε's variable	Drifts

So far, we prefer version 3, although it is hard to obtain because of difficulty of fabrication The insert version allow rotation of the insert and the fractional order of the referee pattern

The referee insert should be thick enough to have a velocity per fringe about 30% different from that of the main cavity, so that at most one main fringe will be obscured by a referee fringe during a dynamic record The 22 mm insert shown for the 6 cm cavity in fig 5 is the thinnest we would advise A 30 mm insert would be better Note from comparing figures 5 and 6 that for stepped version 2, the referee fringes are closer together than those for the main cavity For Version 3 the situation is opposite Also for Version 2, if a referee and main coincide at zero velocity, they will coincide throughout the entire velocity-time record A solid glass pair in a round-about configuration would have a pattern similar to fig 6

7 ACKNOWLEDGMENT

All of these interferometer versions have been used in experiments by George Avara, whose verification of the accuracy of the theory by analsying experiments is greatly appreciated.

8 REFERENCES

1 D R Goosman, "Formulas for Fabry-Perot velocimeter performance using both stripe and multifrequency techniques", Appl Opt. 30(27),3907-3923 (1991)

2 D R Goosman, G Avara, L Steinmetz, C Lai and S Perry, "Manybeam velocimeter for fast surfaces", SPIE proceedings on the 22nd Int. Congress on High Speed Photography and Photonics, 2869 1070-1079 (1996)

3 L L Steinmetz, D R Goosman and G R Avara, "A dual, parallel cavity Fabry-Perot Interferometer", SPIE proceedings on the 21st Int Congress on High Speed Photography and Photonics, 2513 380-386 (1994)

4 L M Barker and K W Schuler, "Correction to the velocity-per-fringe relationship for the VISAR interferometer", J Appl Phys 45, 3692 (1974)

5 C F McMillan, N L Parker and D R Goosman, "Efficiency enhancements for Fabry-Perots used in velocimetry", Appl Opt 28(5), 826-827 (1989)

Work performed under the auspices of the U S Department of Energy by Lawrence Livermore National Laboratory under Contract W-7405-ENG-48

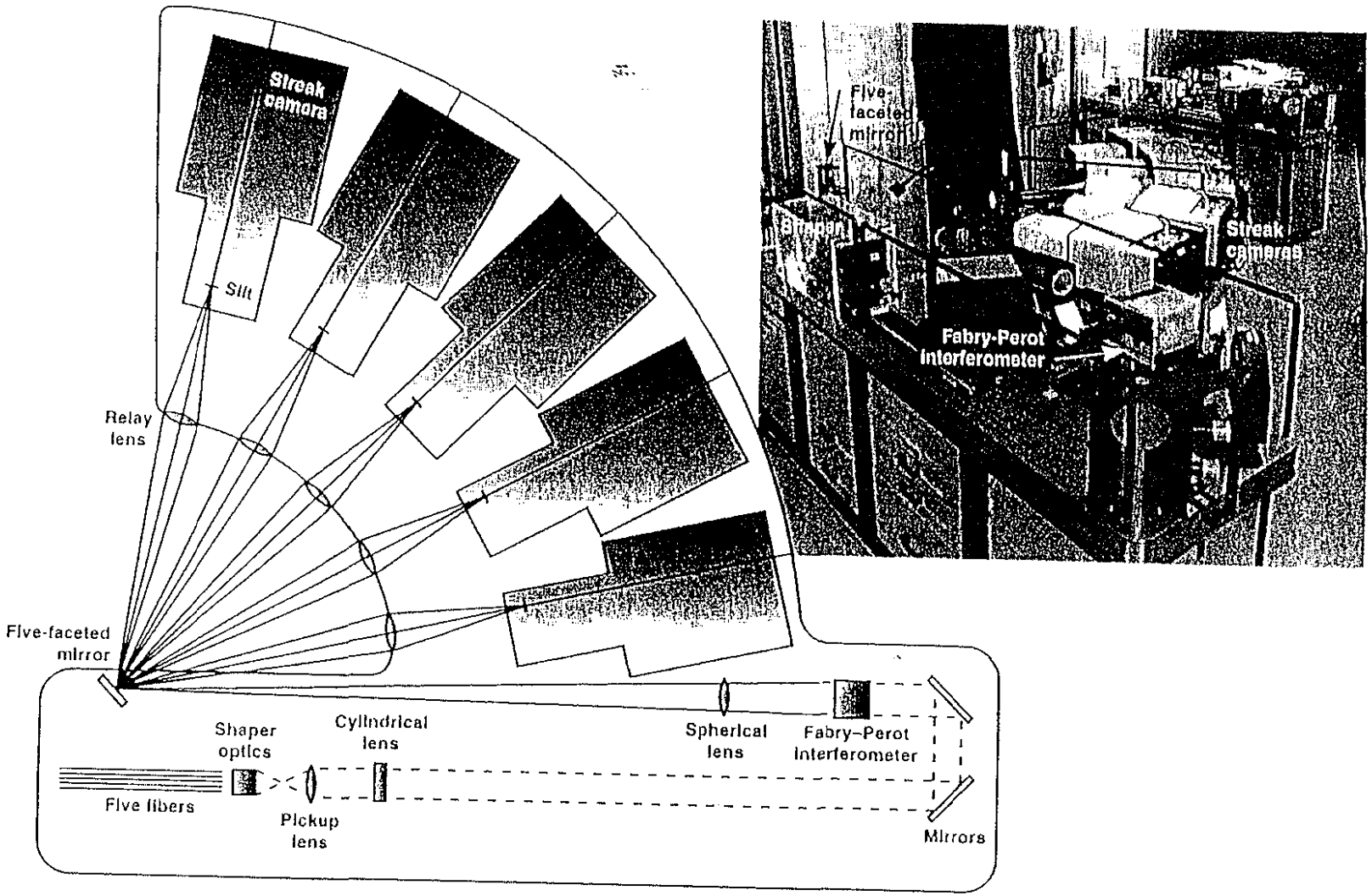

Fig. 1. The major components of the five-beam table, and the actual 10 beam velocimeter.

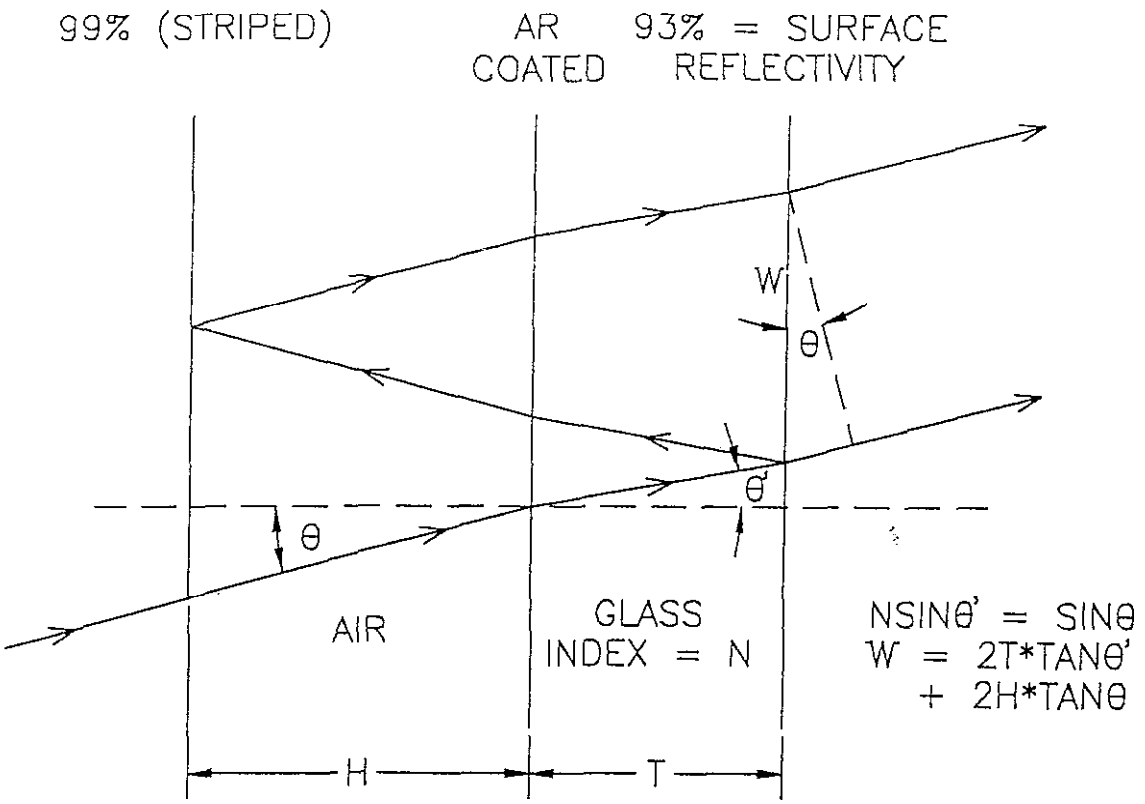

Fig 2 Ray tracing through a cavity consisting of air of length H and glass of index n(λ) and length T

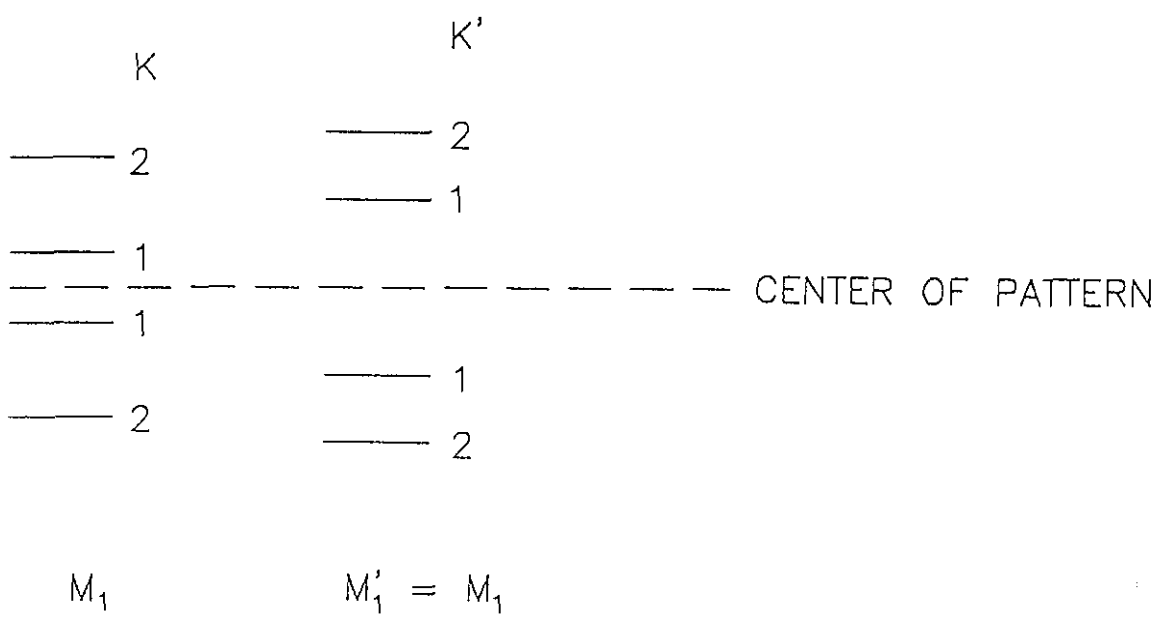

Fig 3 Fringe pattern before (k) and after (k') a small velocity change

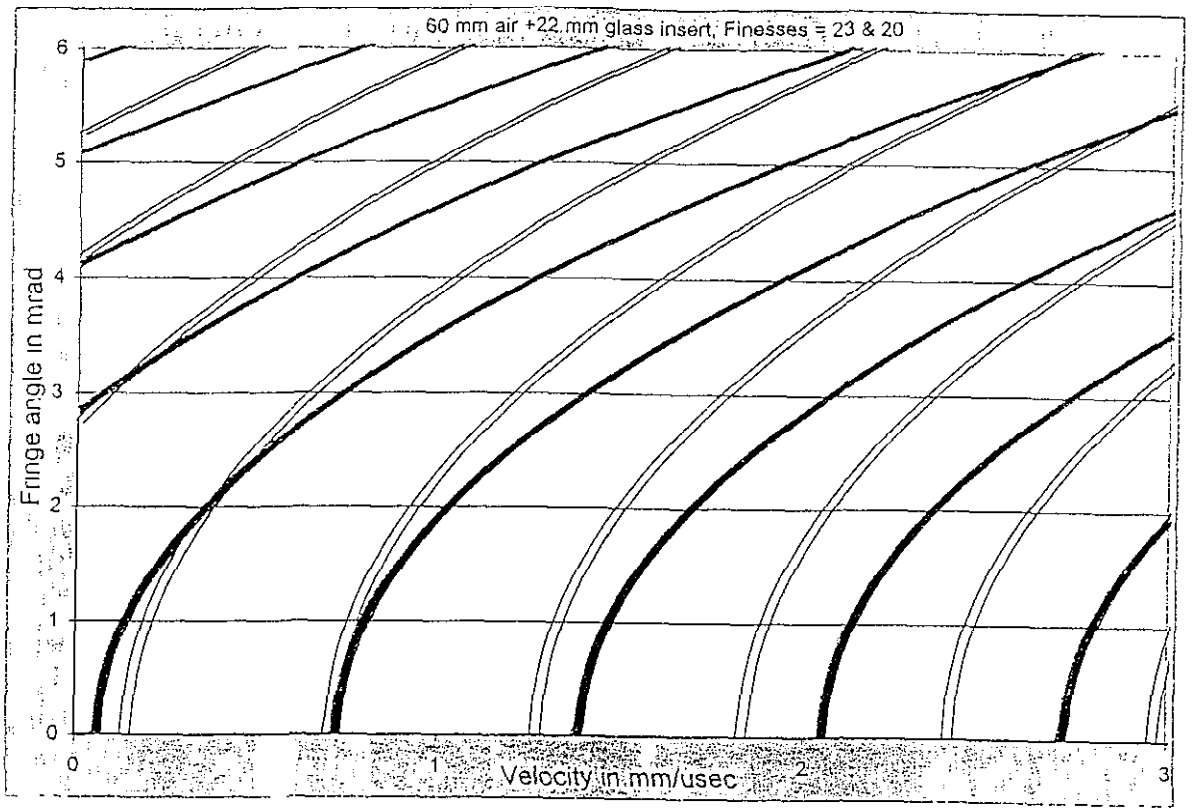

Fig 4 Fringe angle vs velocity for the main (solid line) and referee cavities, with H = 60mm and T = 22 mm. The width of the curves represents the FHWM of the lines for the finesses shown

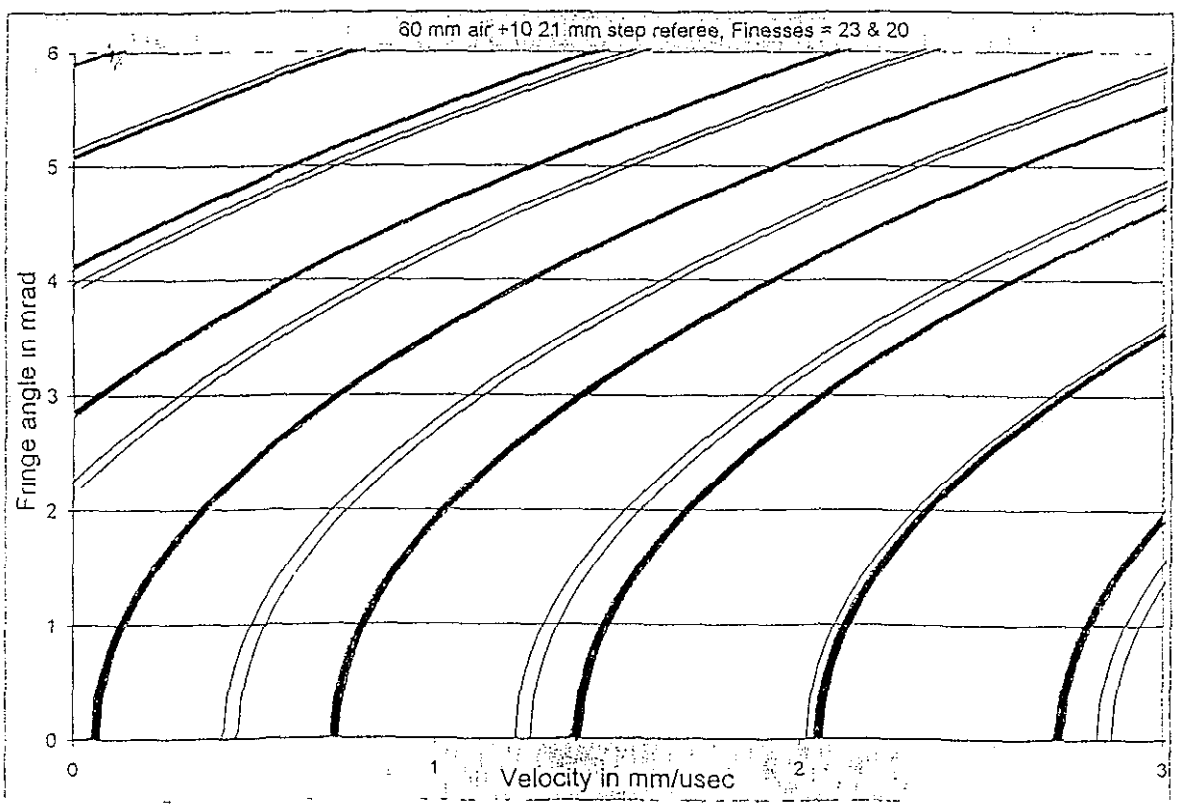

Fig 5 Fringe angle vs velocity for the Version II interferometer with H1=60mm, H2 = 49 79mm

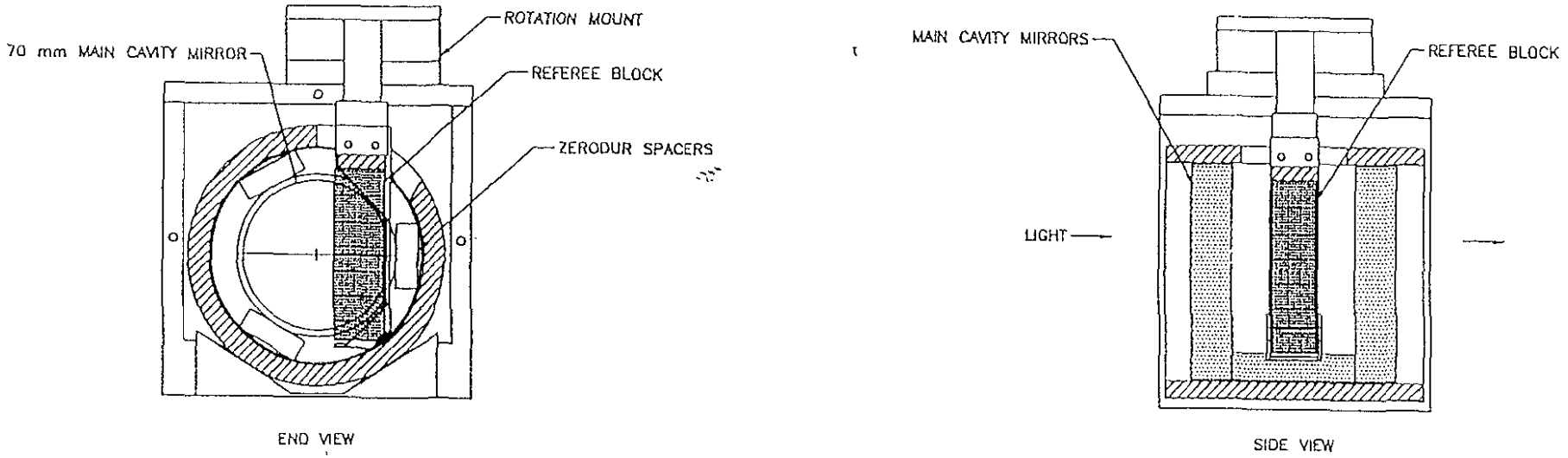

Fig. 6 The version 3 system. Two 70 mm clear aperture plates are separated by 58 mm by three stacks of zerodur spacers. A rotatable solid fused-silica AR coated 20mm referee block is suspended from the top.

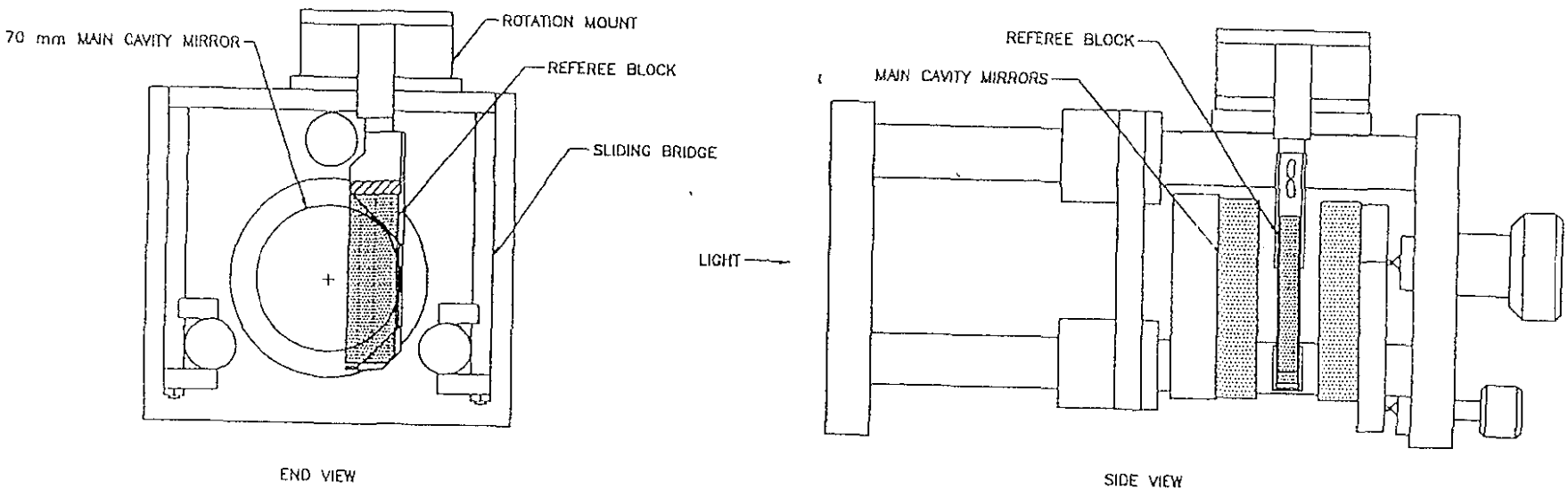

Fig. 7 The version 5 system, which is sliding bridge holding a rotatable 9 mm glass insert over a piezo-driven 70 mm aperture interferometer. A single bridge can be easily transferred to another interferometer.

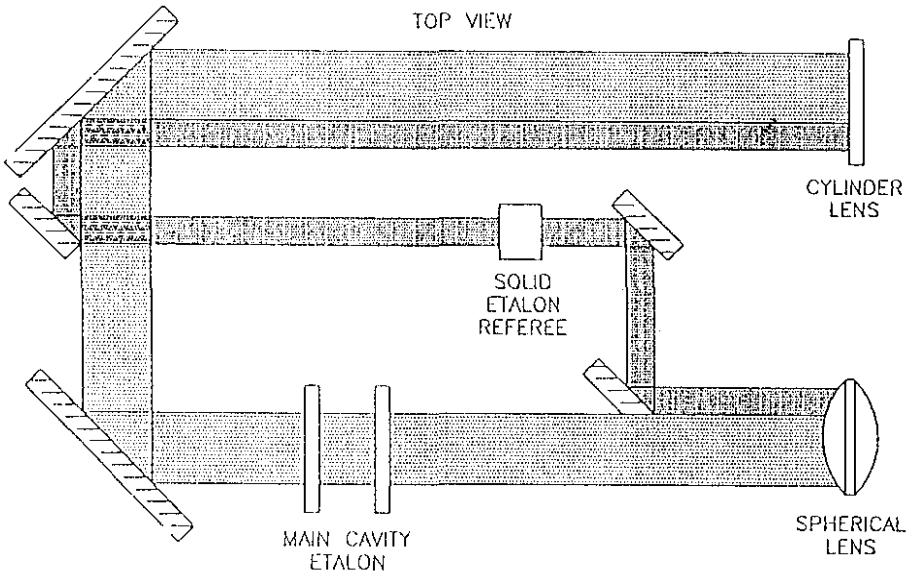

Fig. 8 The round-about configuration for separated main and referee cavities.

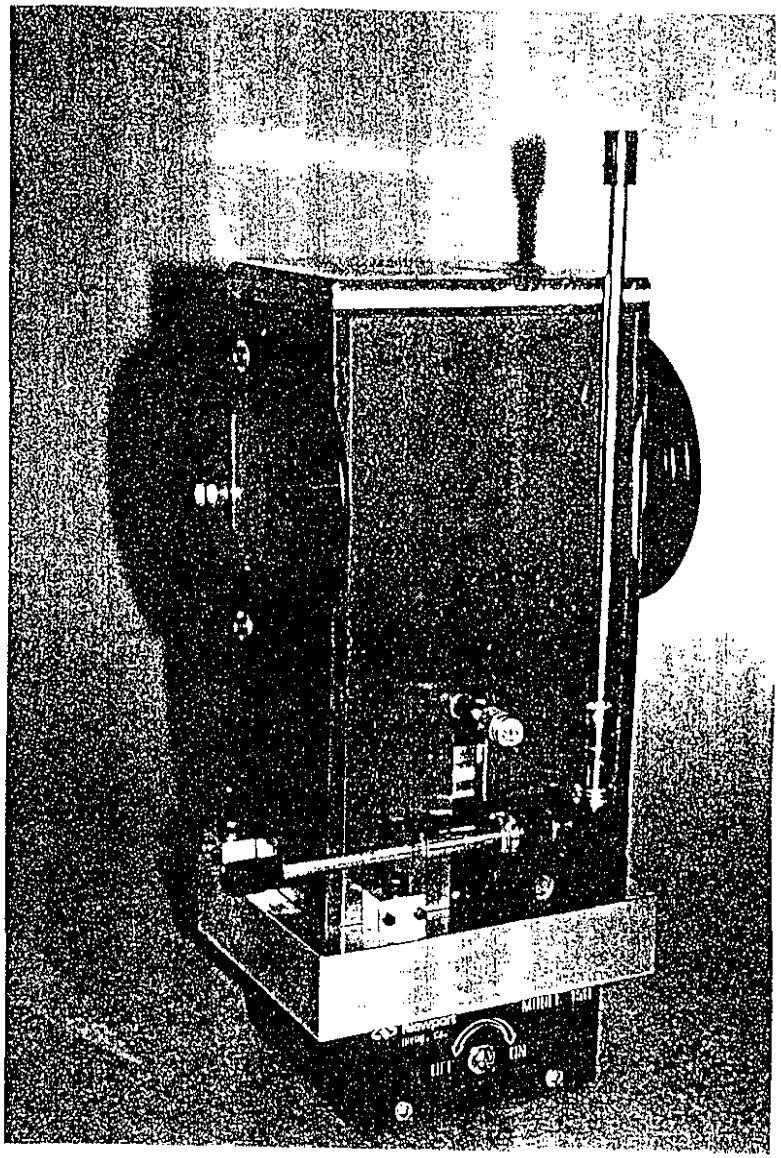

Fig. 9 The massive thermal housing necessary for the version 4 solid etalons. The insulative cover made of aluminum-clad bubble pack has been removed for clarity